

Pyrazoloadenine Inhibitors of the RET Lung Cancer Oncoprotein Discovered by a Fragment Optimization Approach

Debasmita Saha,^[a] Katie Rose Ryan,^[b] Naga Rajiv Lakkaniga,^[a, c] Erica Lane Smith,^[a] and Brendan Frett^{*[a]}

A fragment-based drug-discovery approach was used on a pyrazoloadenine fragment library to uncover new molecules that target the RET (REarranged during Transfection) oncoprotein, which is a driver oncoprotein in ~2% of non-small-cell lung cancers. The fragment library was screened against the RET kinase and LC-2/ad (RET-driven), KM-12 (TRKA-driven matched control) and A549 (cytotoxic control) cells to identify selective scaffolds that could inhibit RET-driven growth. An unsubstituted pyrazoloadenine fragment was found to be active on RET in a biochemical assay, but reduced cell viability in non-RET-driven cell lines (EC_{50} = 1 and 3 μ M, respectively). To increase selectivity for RET, the pyrazoloadenine was modeled in the RET active site, and two domains were identified that were probed with pyrazoloadenine fragment derivatives to improve RET affinity. Scaffolds at each domain were merged to generate a novel lead compound, **8p**, which exhibited improved activity and selectivity for the RET oncoprotein ($A549$ EC_{50} = 5.92 μ M, $LC-2/ad$ EC_{50} = 0.016 μ M, RET IC_{50} = 0.000326 μ M).

Introduction

The RET (REarranged during Transfection) proto-oncogene^[1] encodes a transmembrane receptor tyrosine kinase, which is responsible for activating numerous signalling cascades.^[2] Initially, RET was identified as a driver oncogene in thyroid cancers.^[3] RET mutations were subsequently identified in other cancers^[4] and were found to drive ~2% of non-small-cell lung cancers (NSCLC). Several RET gene fusions have been identified in lung adenocarcinomas and inhibition of these fusions impair

lung cancer growth.^[5] To target RET fusions, small molecule kinase inhibitors have been developed to obstruct RET signalling. Vandetanib and cabozantinib, with FDA approval for thyroid cancer, are in phase II clinical trials for RET-rearranged NSCLC (NCT 01639508 for cabozantinib, NCT 01823068 for vandetanib).^[6–9]

Pyrazoloadenines, with appropriate structural attributes, inhibit a wide range of protein kinases such as BTK (Bruton's tyrosine kinase), CDK1/2 (cyclin-dependent kinase 1/2), Src kinase, and RIPK1 (receptor-interacting protein kinase).^[10–13] Modification of pyrazoloadenine has generated RET inhibitors for papillary thyroid cancer (PTC) for example, PP1 and PP2 (Figure S1 in the Supporting Information).^[14,15] Perceiving the plasticity of pyrazoloadenines, we sought to use a pyrazoloadenine fragment library to test a fragment-based discovery approach by screening the library against the RET kinase. With our prior interest in developing kinase inhibitors,^[16–19] a pyrazoloadenine-based fragment library was screened against RET in biochemical assays as well as cellular assays employing LC-2/ad, a RET-CCDC6 fusion-driven NSCLC cell line, and matched controls to determine oncoprotein specificity (TRK-driven, KM-12) and cytotoxicity (A549). This approach led to the discovery of **8p**, a highly potent and selective pyrazoloadenine-based inhibitor of RET.

Chemistry

In Scheme S1, pyrazoloadenine **1** was iodinated by using *N*-iodosuccinimide in DMF heated to 85 °C for 18 hours to form **2**. Iodinated intermediate **2** was then *N*-alkylated at the N1-pyrazole using different alkyl iodides or bromides in the presence of K_2CO_3 in DMF at 80 °C for 12 hours. Fragments **3b–d** were synthesized by reacting **2** with the respective hydrochloride salt of the alkyl chloride using NaH in dry DMF under inert atmosphere and heated to 80 °C for 24–48 hours. Reacting intermediate **2** with 1-bromo-4-(methylsulfonyl)benzene under copper catalysis produced compound **3d**.

C-3-substituted 1-methyl-1*H*-pyrazolo[3,4-*d*]pyrimidin-4-amines **4a–d** were obtained by reacting **3a** with the corresponding boronic acid using Pd(dppf)Cl₂.DCM complex and K_3PO_4 in dioxane/H₂O (4:1) under microwave irradiation for 1 hour at 100 °C (Scheme S2).

Suzuki coupling of **3a–k** with ethyl 2-(4-(4,4,5,5-tetramethyl-1,3,2-dioxaborolan-2-yl)phenyl)acetate provided fragments **6a–e**. The ester was subjected to saponification by LiOH in THF/H₂O

[a] Dr. D. Saha, Dr. N. R. Lakkaniga, E. L. Smith, Dr. B. Frett
Department of Pharmaceutical Sciences
College of Pharmacy
University of Arkansas for Medical Sciences
Little Rock, AR 72205 (USA)
E-mail: BAFrett@uams.edu

[b] Dr. K. R. Ryan
Department of Biochemistry and Molecular Biology
College of Medicine
University of Arkansas for Medical Sciences
Little Rock, AR 72205 (USA)

[c] Dr. N. R. Lakkaniga
SmartBio Labs
126, Rajamannar Salai, K. K. nagar, Tamilnadu, Chennai-600078 India.

Supporting information for this article is available on the WWW under <https://doi.org/10.1002/cmdc.202100013>

(1:1) under microwave irradiation to generate intermediates **7a–c**. The acid component was subsequently coupled to various heterocyclic amines to afford the pyrazolo[3,4-*d*]pyrimidin-3-yl)phenyl) acetamide derivatives (Scheme S3). Derivative **8s** was synthesized according to the synthetic route depicted in Scheme S4. Reaction of 4-(4,4,5,5-tetramethyl-1,3,2-dioxaborolan-2-yl) aniline with triphosgene in presence of triethylamine in THF at 60 °C for 6 hours provided the isocyanate **10**. Subsequent addition of 5-(*tert*-butyl)isoxazol-3-amine to intermediate **10** provided 1-(5-(*tert*-butyl)isoxazol-3-yl)-3-(4-(4,4,5,5-tetramethyl-1,3,2-dioxaborolan-2-yl)phenyl)urea **11** which was subjected to Suzuki coupling to furnish the derivative **8s**.

Results and Discussion

Inhibitor design by a fragment-based optimization approach

The pyrazoloadenine warhead (fragment **1**) was subjected to a biochemical screen (RET and TRKA) and an oncogene-driven cellular screen (LC-2ad and KM-12). TRKA was employed as an oncoprotein control because of its similarity to the RET kinase domain;^[20] if compounds exhibit selectivity against TRKA, this suggests selectivity in the greater kinome. The biochemical screen indicated selectivity of fragment **1** for RET (RET IC₅₀ = 9.20 μM) over TRK (TRKA IC₅₀ = 57.07 μM). However, the fragment was found to reduce cell viability in both oncogene-driven cell lines (EC₅₀ = 1.47 μM and 1.73 μM, respectively for LC-2ad and KM-12) along with A549 (EC₅₀ = 3.02 μM; cytotoxic control). Despite exhibiting biochemical relevance, fragment **1** was found to be too cytotoxic by nonselectively reducing cell viability, suggesting the fragment did not possess oncoprotein selectivity. To remove the cytotoxicity profile, fragment **1** was visualized in the RET active site to identify ligand-protein interactions to improve affinity (Figure S2).

Fragment **1** was modeled in a RET DFG-out homology model since molecules that interact with the DFG-out fold of RET possess improved selectivity.^[21] By analyzing ligand-protein interactions, it was found that fragment **1** formed two hydrogen bonds with hinge residues Ala807 and Glu805 and π-π interactions with Phe893 at the DFG-motif (Figure S2). The modeling study suggested the possibility for fragment expansion at the solvent front (Domain II) and the allosteric pocket (Domain I; Figure S2). Using modeling insight, fragment **1** underwent expansion at the R¹ position. To probe interactions at the solvent front (Domain II), several pyrazoloadenines fragment derivatives were generated (Table S1). *N*-Methyl substitution slightly improved potency against RET (RET IC₅₀ = 3.3 μM; LC-2/ad EC₅₀ = 1 μM) but was still cytotoxic (A549 EC₅₀ = 1 μM). Introducing polar groups, such as morpholino ethyl **3b** and *N,N*-dimethylethyl **3c**, improved RET activity and lowered cytotoxicity but cell activity diminished likely from permeability issues. Substituting with aromatic groups such as 2-methyl pyridine **3e** and 4-(methylsulfonyl)benzene **3d** decreased potency, whereas propanenitrile **3j** and methoxyethane **3h** drastically reduced activity (Table S1). On the other hand, *N*-

substitution with terminal alcohol **3g**, isopentane **3i**, pyran **3k**, and 3-methoxypropane **3f** improved RET potency and selectivity against TRKA. Of these, 3-methoxypropane (**3f**; RET IC₅₀ = 1.9 ± 2.81 μM) was found to be the most potent in reducing cell viability with 50-fold selectivity over TRKA.

To probe interactions in the kinase back pocket of RET (Domain I), C-3 pyrazoloadenines fragment derivatives were generated (Table S2). All substitutions off the C-3 carbon were found selective for RET over TRKA (**4a–d**). Of these, phenyl **4a** (RET IC₅₀ = 6.82 ± 2.22 μM) and 1-methyl-1*H*-pyrazole **4d** (RET IC₅₀ = 1.044 ± 0.27 μM) were most potent. Analyzing **4a** and **4d** in the RET active site revealed that the phenyl ring of **4a** accesses the RET back pocket through a π-π interaction with Phe893 of the DFG-out motif, while the pyrazole of **4d** did not; hence **4a** was considered for additional modification to better exploit Domain I (Figure S3). To further develop the pyrazoloadenine SAR, derivatives were synthesized to expand into the back pocket of RET. **6a** and **6e** were found to be most active against RET with TRKA selectivity, albeit without cell activity.

The pyrazoloadenine SAR was further developed by modifying substituents in the back pocket (Domain I) while simultaneously altering groups at the solvent front (**6a–e**, **7a–c**; Domain II; Table S3). Among these **6a**, its acidic derivative **7a**, and the *N*-pyran-substituted derivative **6e** were most active. Extension of the aryl substituent at the C-3 position, *via* a carboxylic acid handle, facilitated the exploration of the RET allosteric pocket. A small library of pyrazoloadenine acetamides were synthesized using different aromatic and heterocyclic amines to investigate this pocket (Tables 1 and S4).

In general, when R¹ was methyl pyridine, modification with aryl and heteroaryl amines yielded compounds with weak activity (**8i**, **j**). However, when R³ was 3-cyclopropyl-*N*-methyl pyrazol-5-amine (**8m**), 3-(*tert*-butyl)-*N*-methyl pyrazol-5-amine (**8l**), or 3-(trifluoromethyl)aniline (**8k**) compounds exhibited improved cellular activities consistent with enzymatic activities. Solubilizing groups, such as morpholino ethyl (**8n**), exhibited decent RET inhibition but weak cellular activity, whereas *N,N*-dimethylethyl (**8o**) had diminished RET activity and very poor cellular activity.

A set of pyrazolo pyrimido phenylacetamides (**8a–m**) were synthesized to further define the SAR at the RET back pocket (Tables 1 and S4). Amide modifications with aromatic amines, such as 3-(fluoromethyl)aniline (**8a**), exhibited reduced RET inhibition (RET IC₅₀ = 35.5 μM) in spite maintaining cellular activity (LC-2/ad EC₅₀ = 1.68 μM), whereas 3-(trifluoromethyl)aniline (**8c**) exhibited RET inhibition (RET IC₅₀ = 0.0562 μM) consistent with cellular activity (LC-2/ad EC₅₀ = 0.37 μM). Five-membered heterocyclic amines, 3-(*tert*-butyl)pyrazol-5-amine (**8d**) and 3-(*tert*-butyl)-1-isopropyl pyrazol-5-amine (**8f**), exhibited RET inhibition consistent with cellular activity. While 3-cyclopropyl pyrazol-5-amine (**8e**) exhibited selectivity for RET over TRKA, the analogue had very poor cellular activity, whereas 3-(*tert*-butyl)-1-cyclohexyl pyrazol-5-amine (**8h**) exhibited inhibition of both RET and TRKA while maintaining cellular activity. When 5-(*tert*-butyl) isoxazol-3-amine (**8b**) was utilized as the amine input, the compound exhibited selectivity for RET over TRKA (RET IC₅₀ = 0.00057 μM; TRKA IC₅₀ = 0.202 μM). These

Table 1. Inhibition values and SAR for various N-functionalized substituted phenylacetamides.^[a]

Code	R ¹	R ³	IC ₅₀ [μM]				
			RET	TRKA	LC-2/ad	KM-12	A549
8a	methyl	3-fluoroaniline	35.52 ± 1.41	3.7 ± 0.25	1.68 ± 0.45	2.11 ± 0.08	9.20 ± 3.11
8b	methyl	5-(<i>tert</i> -butyl)-isoxazol-3	0.00057 ± 0.00005	0.20 ± 0.74	0.024 ± 0.02	0.71 ± 0.07	20.35 ± 0.51
8c	methyl	<i>N</i> -methyl-3-(trifluoromethyl)aniline	0.0562 ± 0.000004	4.03 ± 0.93	0.37 ± 0.04	2 ± 0.03	56.3 ± 5.91
8h	methyl	3-(<i>tert</i> -butyl)-1-cyclohexyl- <i>N</i> -methyl-1 <i>H</i> -pyrazol	0.109 ± 0.40	0.295 ± 0.16	1.56 ± 0.36	10.46 ± 0.21	> 20
8k	2-ethylpyridyl	3-(trifluoromethyl) aniline	0.13 ± 0.07	4.74 ± 1.45	0.38 ± 0.03	1.12 ± 0.12	> 20
8l	2-ethylpyridyl	3-(<i>tert</i> -butyl)-1-methyl-1 <i>H</i> -pyrazol	0.069 ± 0.004	3.95 ± 0.8	3.0 ± 0.04	2.57 ± 0.64	> 20
8m	2-ethylpyridyl	3-cyclopropyl-1-methyl-1 <i>H</i> -pyrazol-5-yl	2.93 ± 0.5	0.49 ± 0.18	> 20	> 20	> 20
8n	4-ethylmorpho- line	5-(<i>tert</i> -butyl)isoxazol	0.08 ± 0.02	0.12 ± 0.06	7.83 ± 0.80	> 20	> 20
8p	1-methoxypropyl	5-(<i>tert</i> -butyl)isoxazol	0.000326 ± 0.00005	0.198 ± 0.067	0.016	0.3 ± 0.02	5.92 ± 1.33
8q	1-methoxypropyl	3-fluoro-aniline	0.25 ± 0.07	1.74 ± 0.43	2.41 ± 0.16	4.38 ± 0.30	> 20
8r	1-isobutyl	3-fluoro-aniline	3.48 ± 0.42	2.48 ± 0.83	> 20	> 20	> 20

[a] All data represent means of at least $n=3$ independent experiments.

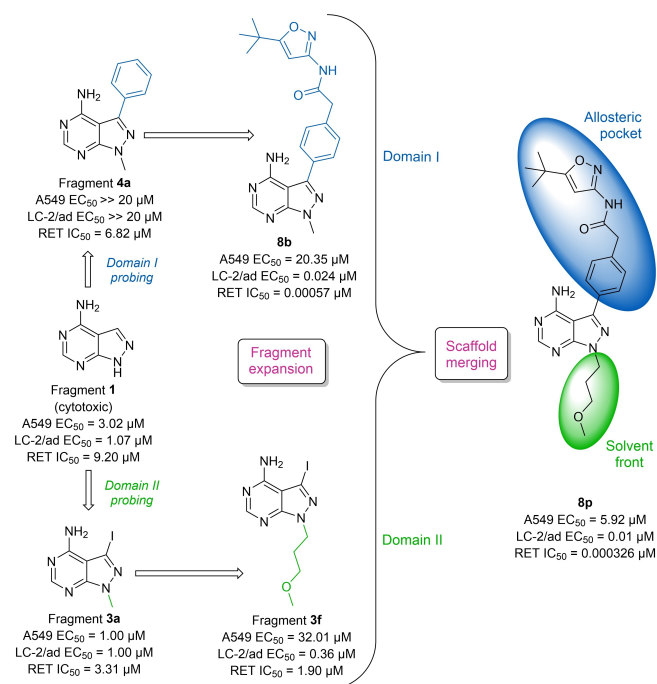
results displayed that the phenyl isoxazole acetamide derivative **8b** possessed notable potency against RET-driven lung cancer with a wide therapeutic window (A549 EC₅₀ = 20.52 μM).

Our previous observations from Table S1 suggested that N-substitutions with isopentane, pyran, and 3-methoxypropane provided improved RET potency and selectivity over TRKA; hence pyrazolo[3,4-*d*]pyrimidin-3-yl phenylacetamide derivatives with *N*-alkyl groups were synthesized and screened. 3-Fluorophenyl acetamide (**8r**) with 1-isobutyl as the *N*-alkyl group exhibited greater TRKA inhibition over RET albeit with poor cellular activity.

On the other hand, 3-fluorophenylacetamide **8q** with 3-methoxypropyl as the *N*-alkyl substituent inhibited RET without selectivity. Hence, after extensive SAR development from the initial fragment 1, it was identified that fragment 3f and compound **8b** exhibited greatest RET selectivity with reduced cytotoxicity. Merging 3f and **8b** into a single molecule generated **8p**. The core of **8p** was identified from the initial biochemical screen and interactions at both the solvent and back pocket of RET were optimized by expanding fragment 1. Merging 3f and **8b** resulted in a twofold improvement in RET potency and cellular activity (LC-2/ad EC₅₀ = 0.01 μM; Figure 1).

Global kinase selectivity of **8p** was assessed using a 97-kinase panel with three RET point mutations at a concentration of 20 nM. The results indicate that **8p** exhibits excellent selectivity with a 0.10 S35 value defined as the percentage of the kinases showing >90% inhibition out of the total number of kinases profiled (Figure S4). Interestingly, **8p** was also found to have high affinity for mutant forms of RET including RETM918T, RETV804L, and RETV804M.

To gain insight into the binding of **8p**, *in-silico* docking studies were performed with the RET kinase DFG [Asp892, Phe893, Gly894]-out computational model (Figure 2). The binding of **8p** to the RET DFG-out form of the kinase suggests **8p** is a type-2 inhibitor.^[21] The pyrazolopyrimidine core of **8p** hydro-

**Figure 1.** Scaffold development strategy that led to RET inhibitor **8p**.

gen bonds with Ala807 and Glu805 at the hinge region. Pyrazoloadenine and the phenyl linker π - π stack with Phe893 of the DFG-motif. The 3-methoxypropane substituent orients towards the solvent front whereas the amide linker and oxygen of the isoxazole moiety form two hydrogen bonds with the backbone atoms of Asp892. This interaction permits access into the allosteric pocket, which is occupied by *tert*-butyl isoxazole.

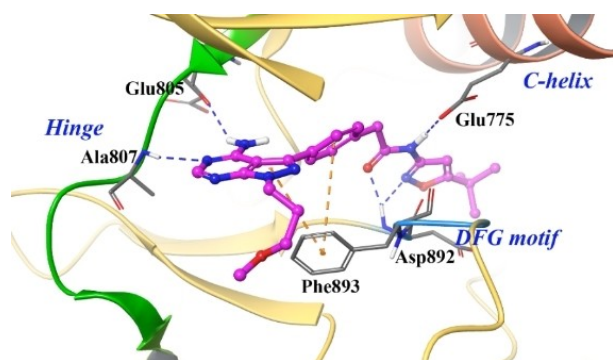


Figure 2. Computational modeling of **8p** in a RET DFG-out homology model. Hydrogen bonds are illustrated in blue and π - π stacking interactions in brown.

Conclusion

This study used a fragment-optimization approach, based on both biochemical and cell-based screens, along with computational studies to identify selective, pyzoloadenine-based RET inhibitors. Modeling uncovered two domains for fragment expansion to probe interactions within the RET active site. SAR studies led to the discovery of **8p**, which is a selective RET inhibitor with sub-nanomolar IC_{50} values against RET ($IC_{50} = 0.00032 \mu\text{M}$) and high potency against LC-2/ad cells ($EC_{50} = 0.01 \mu\text{M}$). Kinome-wide selectivity profiling revealed that **8p** exhibits excellent selectivity for RET and RET mutants over other similar kinases. In conclusion, this research illustrates the usefulness of an fragment-based optimization approach to rapidly probe an active site to refine a promiscuous molecule for a specific kinase oncoprotein.

Acknowledgements

This work was supported by the National Institutes of General Medical Sciences (P20GM109005), a grant from the American Thyroid Association, a UAMS College of Pharmacy Seed grant, and a 2020 UAMS College of Pharmacy Summer Research Fellowship.

Conflict of Interest

The authors declare no conflict of interest.

Keywords: fragment-based drug discovery · oncoproteins · pyzoloadenines · RET inhibitor

- [1] T. A. Attie-Bitach, M. Abitol, M. Gerard, A. L. Delezoide, J. Auge, A. Pelet, J. Amiel, V. Pachnis, A. Munnich, S. Lyonnet, M. Vekemans, *Am. J. Med. Genet.* **1998**, *80*, 481–486.
- [2] E. B. Arighi, M. G. Borrello, H. Sariola, *Cytokine Growth Factor Rev.* **2005**, *16*, 441–467.
- [3] M. Santoro, R. M. Melillo, F. Carlomagno, G. Vecchio, A. Fusco, *Endocrinology*, **2004**, *145*, 448–5451.
- [4] T. Kohno, J. Tabata, T. Nakaoku, *Carcinogenesis* **2020**, *41*, 123–129.
- [5] T. Kohno, H. Ichikawa, Y. Totoki, K. Yasuda, M. Hiramoto, T. Nammo, H. Sakamoto, K. Tsuta, K. Furuta, Y. Shimada, R. Iwakawa, H. Ogiwara, T. Oike, M. Enari, A. J. Schetter, H. Okayama, A. Haugen, V. Skaug, S. Chiku, I. Yamanaka, Y. Arai, S. Watanabe, I. Sekine, S. Ogawa, C. C. Harris, H. Tsuda, T. Yoshida, J. Yokota, T. Shibata, *Nat. Med.* **2012**, *18*, 375–377.
- [6] T. K. Choueiri, S. K. Pal, D. F. McDermott, S. Morrissey, K. C. Ferguson, J. Holland, W. G. Kaelin, J. P. Dutcher, *Ann. Oncol.* **2014**, *25*, 1603–1608.
- [7] W. X. Qi, Z. Shen, F. Lin, Y. J. Sun, D. L. Min, L. N. Tang, A. N. He, Y. Yao, *Br. J. Clin. Pharmacol.* **2013**, *75*, 919–930.
- [8] J. Zang, S. Wu, L. Tang, X. Xu, J. Bai, C. Ding, Y. Chang, L. Yue, E. Kang, J. He, *PLoS One* **2012**, *7*, e30352.
- [9] Z. F. Zhang, T. Wang, L. H. Liu, H. Q. Guo, *PLoS One* **2014**, *9*, e90135.
- [10] F. Rana, Y. Liub, S. Yua, K. Guoa, W. Tanga, X. Chena, G. Zhaoa, *Bioorg. Chem.* **2020**, *94*, 103367.
- [11] L. A. Honigberg, A. M. Smith, M. Sirisawad, E. Verner, D. Loury, B. Chang, S. Li, Z. Pan, D. H. Thamm, R. A. Miller, J. J. Buggy, *Proc. Natl. Acad. Sci. USA* **2010**, *107*, 13075–13080.
- [12] S. Cherukupalli, B. Chandrasekaran, V. Kryštof, R. R. Aleti, N. Sayyad, S. R. Merugu, N. D. Kushwaha, R. Karpoornath, *Bioorg. Chem.* **2018**, *79*, 46–59.
- [13] Y. Li, Y. Xiong, G. Zhang, L. Zhang, W. Yang, J. Yang, L. Huang, Z. Qiao, Z. Miao, G. Lin, Q. Sun, T. Niu, L. Chen, D. Niu, L. Li, S. Yang, *J. Med. Chem.* **2018**, *61*, 11398–11414.
- [14] F. Carlomagno, D. Vitagliano, T. Guida, M. Napolitano, G. Vecchio, A. Fusco, A. Gazit, A. Levitzki, M. Santoro, *Cancer Res.* **2002**, *62*, 1077–1082.
- [15] P. Dinér, J. P. Alao, J. Söderlund, P. Sunnerhagen, M. Grötl, *J. Med. Chem.* **2012**, *55*, 4872–4876.
- [16] D. Saha, A. Kharbanda, W. Yan, N. R. Lakkaniga, B. Frett, H.-Y. Li, *J. Med. Chem.* **2020**, *63*, 441–469.
- [17] N. R. Lakkaniga, L. Zhang, B. Belachew, N. Gunaganti, B. Frett, H.-Y. Li, *J. Med. Chem.* **2020**, *203*, 112589.
- [18] J. B. Bharate, N. McConnell, G. Naresh, L. Zhang, N. R. Lakkaniga, L. Ding, N. P. Shah, B. Frett, H. Li, *Sci. Rep.* **2018**, *8*, 3722.
- [19] D. Saha, A. Kharbanda, N. Essien, L. Zhang, R. Cooper, D. Basak, S. Kendrick, B. Frett, H.-Y. Li, *Org. Chem. Front.* **2019**, *6*, 2234.
- [20] I. Gudernova, L. Balek, M. Varecha, J. F. Kucerova, M. K. Bosakova, B. Fafilek, V. Palusova, S. Uldrijan, L. Trantirek, P. Krejci, *Oncotarget* **2017**, *65*, 109319.
- [21] B. Frett, F. Carlomagno, M. L. Moccia, A. Brescia, G. Federico, V. D. Falco, B. Admire, Z. Chen, W. Qi, M. Santoro, H. Y. Li, *Angew. Chem. Int. Ed.* **2015**, *54*, 8717.

Manuscript received: January 7, 2021

Revised manuscript received: February 1, 2021

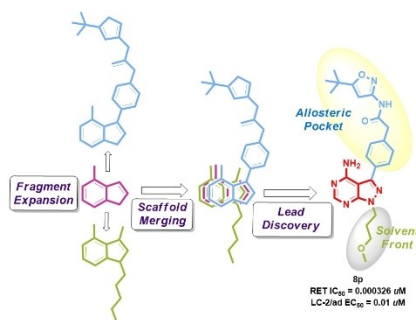
Accepted manuscript online: February 8, 2021

Version of record online: ■■■, ■■■■

COMMUNICATIONS

Refining a promiscuous molecule:

Based on on biochemical and cell-based screens plus computational studies, a fragment-optimization approach was used to identify pyrazoloadenine-based inhibitors of the RET oncoprotein. Modeling uncovered two domains to probe interactions within the RET active site; then SAR studies led to compound **8p**, which exhibits excellent selectivity for RET and RET mutants over other similar kinases.



Dr. D. Saha, Dr. K. R. Ryan, Dr. N. R. Lakkaniga, E. L. Smith, Dr. B. Frett*

1 – 5

Pyrazoloadenine Inhibitors of the RET Lung Cancer Oncoprotein Discovered by a Fragment Optimization Approach

